Chapter 18
Nuclear Energy Production

We shall limit ourselves here to a very rough summary of the most important features of nuclear reactions in stars. This will suffice completely for the consideration of the main band of stellar structures, while the study of particular aspects of nuclear astrophysics anyway requires the consultation of specialized literature (see Clayton 1968, or Iliadis 2007). For example, we will only deal with energy production of equilibrium nuclear burning, i.e. we will neglect the effects occurring when the timescale of a rapidly changing star becomes comparable to that of an important nuclear reaction. On the other hand, we will also briefly touch on such topics as electron screening or neutrino production, about which a certain minimum of information seems to be indispensible for general discussions.

We begin with a few historical comments. That thermonuclear reactions can provide the energy source for the stars was first shown by R. Atkinson and F. Houtermans in 1929, after G. Gamow discovered the tunnel effect. Later, two important discoveries were published almost simultaneously in 1938: H. Bethe and Ch. Critchfield described the *pp* chain, and C.F. von Weizsäcker and Bethe independently found the CNO cycle. The reactions of helium burning were then described in 1952 by E.E. Salpeter. Finally, a classic paper summarized the state of the art in 1957, "Synthesis of the Elements in Stars" (Burbidge et al. 1957).

18.1 Basic Considerations

Most observed stars (including the Sun) live on so-called thermonuclear fusion. In such nuclear reactions, induced by the thermal motion, several lighter nuclei fuse to form a heavier one. Before this process, the involved nuclei j have a total mass ($\sum M_j$) different from that of the product nucleus (M_y). The difference is called the *mass defect*:

$$\Delta M = \sum_j M_j - M_y \ . \tag{18.1}$$

R. Kippenhahn et al., *Stellar Structure and Evolution*, Astronomy and Astrophysics Library, DOI 10.1007/978-3-642-30304-3_18, © Springer-Verlag Berlin Heidelberg 2012

It is converted into energy according to Einstein's formula

$$E = \Delta M c^2 \tag{18.2}$$

and is available (at least partly) for the star's energy balance. An example is the series of reactions called "hydrogen burning", where four hydrogen nuclei ^{1}H with a total mass $4 \times 1.0079\, m_\mathrm{u}$ (atomic mass units, physical scale) are transformed into one ^{4}He nucleus of $4.0026 m_\mathrm{u}$. Atomic masses are given for the neutral atoms, i.e. for the nucleus plus all electrons. However, since the electron mass is only $1/1823\, m_\mathrm{u}$, we will assume that masses of nuclei are the same as the atomic masses. Obviously $2.9 \times 10^{-2} m_\mathrm{u}$ per produced ^{4}He nucleus have "disappeared" during the fusion of the four protons, which is roughly 0.7 % of the original masses and which corresponds to an energy of about 27.0 MeV according to (18.2). As usual in nuclear physics, as the unit of energy, we take the electron volt eV ($1\,\mathrm{eV} = 1.6018 \times 10^{-12}$ erg) with the following equivalences:

$$\begin{aligned} 1\,\mathrm{keV} &\mathrel{\widehat{=}} 1.1606 \times 10^7\,\mathrm{K}\,, \\ 931.49\,\mathrm{MeV} &\mathrel{\widehat{=}} 1\, m_\mathrm{u}\,. \end{aligned} \tag{18.3}$$

The Sun's luminosity corresponds to a mass loss rate of $L_\odot/c^2 = 4.26 \times 10^{12}\,\mathrm{g\,s^{-1}}$, which appears to be a lot, especially if it is read as "more than four million metric tons per second". If a total of 1 $M_\odot$ of hydrogen were converted into ^{4}He, then the disappearing 0.7 % of this mass would be 1.4×10^{31} g, which could balance the Sun's present mass loss by radiation for about 3×10^{18} s $\approx 10^{11}$ years.

The deficiency of mass is just another aspect of the fact that the involved nuclei have different binding energies E_B. This is the energy required to separate the nucleons (protons and neutrons in the nucleus) against their mutual attraction by the strong, but short-range nuclear forces. Or else, E_B is the energy gained if they are brought together from infinity (which starts here at any distance large compared with, say, 10^{-12} cm, the scale of a nuclear size).

Consider a nucleus of mass M_nuc and atomic mass number A (the integer "atomic weight"): it may contain Z protons of mass m_p and $(A - Z)$ neutrons of mass m_n. Its binding energy is then related to these masses by (18.2):

$$E_\mathrm{B} = [(A - Z)m_\mathrm{n} + Z m_\mathrm{p} - M_\mathrm{nuc}]c^2\,. \tag{18.4}$$

When comparing different nuclei, it is more instructive to consider the *average binding energy per nucleon,*

$$f = \frac{E_\mathrm{B}}{A}\,, \tag{18.5}$$

which is also called the *binding fraction*. With the exception of hydrogen, typical values are around 8 MeV, with relatively small differences for nuclei of very different A. This shows that the short-range nuclear forces due to a nucleon mainly affect the nucleons in its immediate neighbourhood only, such that with increasing

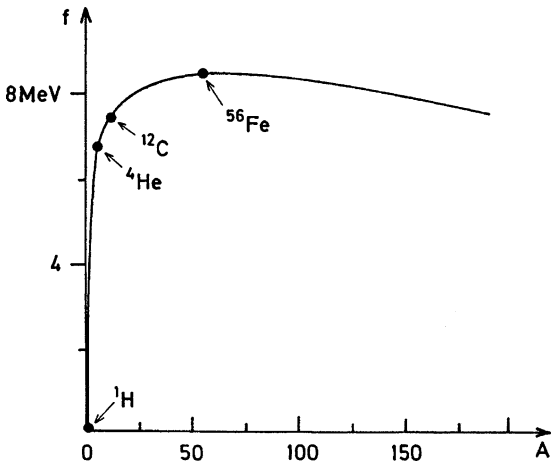

Fig. 18.1 A smoothed run of the fractional binding energy per nucleon, $f = E_B/A$, for stable nuclei, over the atomic mass number A. The curve is smoothed over the wiggles which are due to the nuclear shell structure and pair effects

A, a saturation occurs rather than an increase of f proportional to A. An idealized plot of f against A is shown in Fig. 18.1 (The real curve zigzags around this smoothed curve as a consequence of the shell structure of the nucleus and pair effects.).

With increasing A, $f(A)$ rises steeply from hydrogen, then flattens out and reaches a maximum of 8.5 MeV at $A = 56$ (^{56}Fe), after which it drops slowly with increasing A. The increase for $A < 56$ is a surface effect: particles at the surface of the nucleus experience less attraction by nuclear forces than those in the interior, which are completely surrounded by other particles. And in a densely packed nucleus, the surface area increases with radius slower than the volume (i.e. the number A) such that the fraction of surface particles drops. With increasing A, the number Z of protons also increases (The addition of neutrons only would require higher energy states, because the Pauli principle excludes more than two identical neutrons, and the nuclei would be unstable.). The positively charged protons experience a repulsive force which is far-reaching and therefore does not show the saturation of the nuclear forces. This increasing repulsion by the Coulomb forces brings the curve in Fig. 18.1 down again for $A > 56$.

Around the maximum, at ^{56}Fe, we have the most tightly bound nuclei. In other words, the nucleus of ^{56}Fe has the smallest mass per nucleon, so that any nuclear reaction bringing the nucleus closer to this maximum will be exothermic, i.e. will release energy. There are two ways of doing this:

1. By fission of heavy nuclei, which happens, for example, in radioactivity.
2. By fusion of light nuclei, which is the prime energy source of stars (and possibly ours too in the future).

Clearly, both reach an end when one tries to extend them over the maximum of f, which is therefore a natural finishing point for the stellar nuclear engine. So if a star initially consisted of pure hydrogen, it could gain a maximum of about 8.5 MeV per

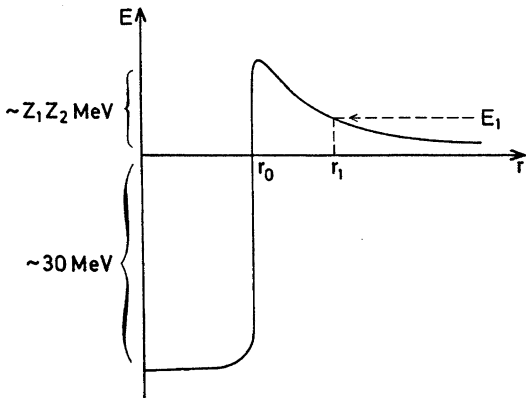

Fig. 18.2 Sketch of the potential over the distance r from the nuclear centre. Nuclear attraction dominates for $r < r_0$ and Coulomb repulsion for $r > r_0$. A particle starting at infinity with kinetic energy E_1 of the relative motion will approach classically only to r_1

nucleon by fusion to ^{56}Fe, but 6.7 MeV of these are already used up when ^{4}He is built up in the first step.

In order to obtain a fusion of charged particles, they have to be brought so close to each other that the strong, but very short-ranged, nuclear forces dominate over the weaker, but far-reaching, Coulomb forces. The counteraction of these two forces leads to a sharp potential jump at the interaction radius (Fig. 18.2):

$$r_0 \approx A^{1/3} 1.44 \times 10^{-13} \text{cm} \tag{18.6}$$

(the "nuclear radius" of the order of femtometer, 1fm $= 10^{-13}$cm). For distances less than r_0, the nuclear attraction dominates and provides a potential drop of roughly 30 MeV, while "outside" r_0, the repulsive Coulomb forces for particles with charges Z_1 and Z_2 yield

$$E_{\text{Coul}} = \frac{Z_1 Z_2 e^2}{r} \,. \tag{18.7}$$

The height of the *Coulomb barrier* $E_{\text{Coul}}\,(r_0)$ is typically of the order

$$E_{\text{Coul}}(r_0) \approx Z_1 Z_2 \,\text{MeV} \,. \tag{18.8}$$

If, in the stationary reference frame of the nucleus, a particle at "infinity" has kinetic energy E_1, it can come classically only to a distance r_1 given by $E_1 = E_{\text{Coul}}(r_1)$ from (18.7), as indicated in Fig. 18.2. Now, the kinetic energy available to particles in stellar interiors is that of their thermal motion, and hence the reactions triggered by this motion are called *thermonuclear*. Since in normal stars we observe a slow energy release rather than a nuclear explosion, we must certainly expect the *average* kinetic energy of the thermal motion, E_{th}, to be considerably smaller than $E_{\text{Coul}}(r_0)$. For the value $T \approx 10^7$ K estimated for the solar centre in Sect. 2.3, according to (18.3), kT is only 10^3 eV, i.e. E_{th} is smaller than the Coulomb barrier (18.8) by a factor of roughly 10^3. This is in fact so low that, with classical effects only, we

can scarcely expect any reaction at all. In the high-energy tail of the Maxwell–Boltzmann distribution, the exponential factor drops here to exp $(-1000) \approx 10^{-434}$, which leaves no chance for the "mere" 10^{57} nucleons in the whole Sun (and even for the $\approx 10^{80}$ nucleons in the whole visible universe)!

The only possibility for thermonuclear reactions in stars comes from a quantum-mechanical effect found by G. Gamow: there is a small but finite probability of penetrating ("tunnelling") through the Coulomb barrier, even for particles with $E < E_{\mathrm{Coul}}(r_0)$. This tunnelling probability varies as

$$P_0 = p_0 E^{-1/2} \mathrm{e}^{-2\pi\eta} \; ; \quad \eta = \left(\frac{m}{2}\right)^{1/2} \frac{Z_1 Z_2 e^2}{\hbar E^{1/2}} \; . \tag{18.9}$$

Here $\hbar$ is $h/2\pi$ and m the reduced mass. The factor p_0 depends only on the properties of the two colliding nuclei. The exponent $2\pi\eta$ is here obtained as the only E-dependent term in an approximate evaluation of the integral over $\hbar^{-1}[2m(E_{\mathrm{Coul}} - E)]^{1/2}$, which is extended from r_0 to the distance r_{c} of closest approach (where $E = E_{\mathrm{Coul}}$). For $Z_1 Z_2 = 1$ and $T = 10^7$ K, P_0 is of the order of 10^{-20} for particles with average kinetic energy E and steeply increases with E and decreases with $Z_1 Z_2$. Therefore, for temperatures as "low" as 10^7 K, only the lightest nuclei (with smallest $Z_1 Z_2$) have a chance to react. For reactions of heavier particles, with larger $Z_1 Z_2$, the energy, i.e. the temperature, has to be correspondingly larger to provide a comparable penetration probability. This will result in well-separated phases of different nuclear "burning" during the star's evolution.

18.2 Nuclear Cross Sections

Consider a reaction of the nucleus X with the particle a by which the nucleus Y and the particle b are formed:

$$a + X \rightarrow Y + b \; , \tag{18.10}$$

represented by the notation *X(a, b)Y*. The reaction probability depends on nuclear details, some of which can be illustrated with the following simplified description. After penetration of the Coulomb barrier, an excited *compound nucleus* C^* may form containing both original particles (The level of excitation is dependent on the kinetic energy and binding energy brought along by the newly added particle.). C^* may decay after a short time, which will still be long enough for the added nucleons to "forget"–owing to interactions within the compound nucleus–their history, a process for which only $\sim 10^{-21}$ s is necessary. The decay then depends only on the energy. C^* can generally decay via one of several "channels" of different probability: $C^* \rightarrow X + a, \rightarrow Y_1 + b_1, \rightarrow Y_2 + b_2, \ldots, \rightarrow C + \gamma$. The first of these would be the reproduction of the original particles, while the last indicates a decay with γ-ray emission; the others are particle decays where the $b_1, b_2, \ldots$ may be, for example, neutrons, protons, and α particles. Compared to these, a decay

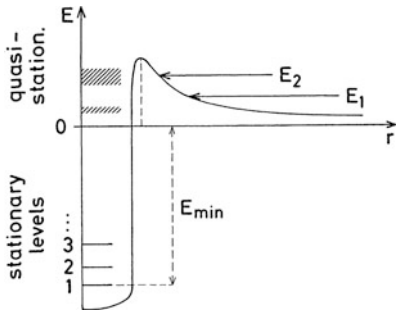

Fig. 18.3 Schematic sketch of energy levels in a compound nucleus C^* formed by particles X and a. The zero of E is here taken as corresponding to zero velocity of X and a at infinity. For initial particle energy E_1, the reaction would be non-resonant, while for E_2, the particles X and a find a resonance in the compound nucleus. $E_{\min}$ is the minimum excitation energy above the ground level for particle emission

with electron emission has negligible probability (β decay times being of order 1 s or larger). Outgoing particles will obtain a certain amount of kinetic energy, which (just as the energy of emitted γ rays) will be shared with the surroundings, though an exception here are the neutrinos, which leave the star without interaction (Sect. 18.7). The possibility that a given energy level of C^* can decay via a certain channel requires fulfilment of the conservation laws (energy, momentum, angular momentum, nuclear symmetries).

It is very important to know the energy levels of the compound nucleus C^*, which can be of different types. Let $E_{\min}$ be the minimum energy required to remove a nucleon from the ground state to infinity with zero velocity (to the level $E = 0$ in Fig. 18.3). This corresponds to the atom ionization energy discussed in Chap. 14. Levels below $E_{\min}$ can obviously only decay by electromagnetic transitions with the emission of γ rays, which are relatively improbable, and hence their lifetime τ is large; these are "stationary" levels of small energy width Γ, since

$$\Gamma = \frac{\hbar}{\tau} , \tag{18.11}$$

as follows from the Heisenberg uncertainty relation. These levels correspond to the discrete, bound atomic states.

The compound nucleus will not, however, immediately expel a particle if its energy is somewhat above $E_{\min}$, since the sharp potential rise holds it back, at least for some time. Eventually it can leave the potential well by the tunnelling effect (which was, in fact, predicted by Gamow for explaining such outward escapes of particles from radioactive nuclei). So there can be "quasi-stationary" levels above $E_{\min}$ that have an appreciably shorter lifetime τ (and are correspondingly wider) than those below $E_{\min}$, since they can also decay via the much more probable particle emission. This probability will clearly increase strongly with increasing energy, which results in corresponding decreases of τ and increases

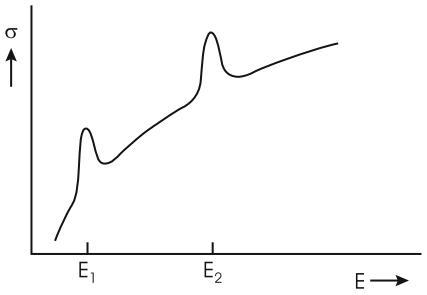

Fig. 18.4 Sketch of the reaction cross section σ over the energy E of the relative motion of the reacting particles, with resonances at E_1 and E_2

of Γ, see (18.11). Above a certain energy $E_{\max}$ the width Γ will become larger than the distance between neighbouring levels, and their complete overlap yields a continuum of energy states, instead of separated, discrete levels.

The possible existence of quasi-stationary levels above $E_{\min}$ requires particular attention. Consider an attempt to produce the compound nucleus C^* by particles $X + a$ with gradually increasing energy E of their relative motion at large distances. The reaction probability will simply increase with the penetration probability (18.9), if E is in a region either without quasi-stationary levels or between two of them. If, however, E coincides with such a level, the colliding particles find a "resonance" and can form the compound nucleus much more easily. At such resonance energies E_{res}, the probability for a reaction (and hence the cross section σ) is abnormally enhanced, as sketched in Fig. 18.4, with resonant peaks rising to several powers of ten above "normal". The energy dependence of the cross section therefore has a factor which has the typical resonance form:

$$\xi(E) = \text{constant}\,\frac{1}{(E - E_{\text{res}})^2 + (\Gamma/2)^2}\,. \tag{18.12}$$

At a resonance, the cross section σ for the reaction of particles X and a can nearly reach its maximum value (geometrical cross section), given by quantum mechanics as $\pi\lambda\!\!\!^{-2}$, where $\lambda\!\!\!^{-}$ is the de Broglie wavelength associated with a particle of relative momentum p:

$$\lambda\!\!\!^{-} = \frac{\hbar}{p} = \frac{\hbar}{(2mE)^{1/2}}\,. \tag{18.13}$$

Here the non-relativistic relation between p and E is used, and m is the reduced mass of the two particles. The meaning of $\pi\lambda\!\!\!^{-2}$ is clear because according to quantum mechanics, the particles moving with momentum p "see" each other not as a precise point but smeared out over a length $\lambda\!\!\!^{-}$. The dependence of σ on E can now be seen from the relation

$$\sigma(E) \sim \pi\lambda\!\!\!^{-2} P_0(E)\xi(E)\,, \tag{18.14}$$

where $\lambda\!\!\!^{-}$ is given by (18.13). For E values well below the Coulomb barrier, P_0 can be taken from (18.9) with a pre-factor $p_0 = E_{\text{Coul}}^{1/2}(r_0)\exp[32mZ_1Z_2e^2r_0/\hbar^2)^{1/2}]$. In the range of a single resonance, $\xi(E)$ is given by (18.12), while far

away from any resonances, $\xi \to 1$. In any case, with or without resonances, σ is proportional to $\lambda\!\!\!^{-2} P_0$, which depends on E as shown by (18.9) and (18.13). Therefore one usually writes

$$\sigma(E) = SE^{-1}\mathrm{e}^{-2\pi\eta} \ , \tag{18.15}$$

where all remaining effects are contained within the here-defined *"astrophysical factor" S*. This factor contains all intrinsic nuclear properties of the reaction under consideration and can, in principle, be calculated, although one rather relies on measurements.

The difficulty with laboratory measurements of $S(E)$–if they are possible at all– is that, because of the small cross sections, they are usually feasible only at rather high energies, say above 0.1 MeV, but this is still roughly a factor 10 larger than those energies which are relevant for astrophysical applications. Therefore one has to extrapolate the measured $S(E)$ downwards over a rather long range of E. This can be done quite reliably for non-resonant reactions, in which case S is nearly constant or a very slowly varying function of E [an advantage of extrapolating $S(E)$ rather than $\sigma(E)$]. The real problems arise from (suspected or unsuspected) resonances in the range over which the extrapolation is to be extended. Then the results can be quite uncertain. Only in underground laboratories, where the experiments are shielded from cosmic rays by hundreds of meters of solid rock, it is sometimes possible to measure the nuclear cross sections of at least a few nuclear reactions at energies as low as 10–30 keV, i.e. at energies relevant for nuclear processes in stellar interiors. The first such measurement was done by Junker et al. (1998) in the *Gran Sasso Laboratory* and concerned the $^3\mathrm{He}(^3\mathrm{He}, 2p)^4\mathrm{He}$ reaction (18.62) of the hydrogen burning chains (Sect. 18.5.1). Such experiments sometimes lead to the discovery of resonances, but more importantly reduce the uncertainties of the cross sections considerably, and confirm the near constancy of $S(E)$ at the relevant energies.

18.3 Thermonuclear Reaction Rates

Let us denote the types of reacting particles, X and a, by indices j and k respectively. Suppose there is one particle of type j moving with a velocity v relative to all particles of type k. Its cross section σ for reactions with the k sweeps over a volume σv per second. The number of reactions per second will then be $n_k \sigma v$ if there are n_k particles of type k per unit volume. For n_j particles per unit volume the total number of reactions per units of volume and time is

$$\tilde{r}_{jk} = n_j n_k \sigma v \ . \tag{18.16}$$

This product may also be interpreted by saying that $n_j n_k$ is the number of pairs of possible reaction partners, and σv gives the reaction probability per pair and

second. This indicates what we have to do in the case of reactions between identical particles ($j = k$). Then the number of pairs that are possible reaction partners is $n_j(n_j - 1)/2 \approx n_j^2/2$ for large particle numbers. This has to replace the product $n_j n_k$ in (18.16) so that we can generally write

$$\tilde{r}_{jk} = \frac{1}{1+\delta_{jk}} n_j n_k \sigma v \ , \quad \delta_{jk} = \begin{cases} 0, \ j \neq k \\ 1, \ j = k \end{cases} . \tag{18.17}$$

Now we have to allow for the fact that particles j and k do not move relatively to each other with uniform velocities, which is important since σ depends strongly on v. Excluding extreme densities (as, e.g. in neutron stars) we can assume that both types have a Maxwell–Boltzmann distribution of their velocities. It is then well known that also their *relative velocity* v is Maxwellian. If the corresponding energy is

$$E = \frac{1}{2} m v^2 \tag{18.18}$$

with the reduced mass $m = m_j m_k/(m_j + m_k)$, the fraction of all pairs contained in the interval $[E, E + dE]$ is given by

$$f(E)dE = \frac{2}{\sqrt{\pi}} \frac{E^{1/2}}{(kT)^{3/2}} \mathrm{e}^{-E/kT} dE \ . \tag{18.19}$$

This fraction of all pairs has a uniform velocity and contributes the amount $dr_{jk} = \tilde{r}_{jk} f(E)dE$ to the total rate. The total reaction rate per units of volume and time is then given by the integral $\int dr_{jk}$ over all energies, which formally can be written as

$$r_{jk} = \frac{1}{1+\delta_{jk}} n_j n_k \langle \sigma v \rangle \ , \tag{18.20}$$

where the averaged probability is

$$\langle \sigma v \rangle = \int_0^\infty \sigma(E) v f(E) dE \ . \tag{18.21}$$

Let us replace the particle numbers per unit volume n_i by the mass fraction X_i with

$$X_i \varrho = n_i m_i \ , \tag{18.22}$$

cf. (8.2). If the energy Q is released per reaction, then (18.20) gives the energy generation rate per units of mass (instead of unit volume; obtained by dividing by ϱ) and time:

$$\varepsilon_{jk} = \frac{1}{1+\delta_{jk}} \frac{Q}{m_j m_k} \varrho X_j X_k \langle \sigma v \rangle \ . \tag{18.23}$$

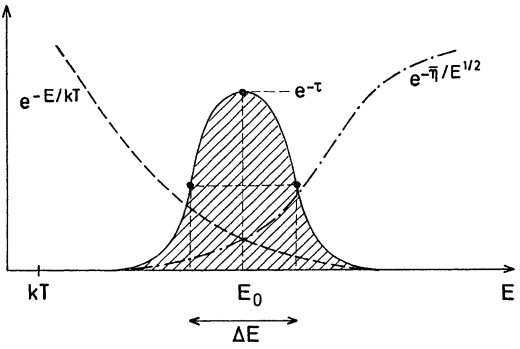

Fig. 18.5 The Gamow peak (*solid curve*) as the product of Maxwell distribution (*dashed*) and penetration factor (*dot-dashed*). The hatched area under the Gamow peak determines the reaction rate. All three curves are on different scales

Using (18.9), (18.15), (18.18) and (18.19) in (18.21), the average cross section $\langle \sigma v \rangle$ can be written as

$$\langle \sigma v \rangle = \frac{2^{3/2}}{(m\pi)^{1/2}} \frac{1}{(kT)^{3/2}} \int_0^\infty S(E) \mathrm{e}^{-E/kT - \bar{\eta}/E^{1/2}} dE \,, \tag{18.24}$$

where

$$\bar{\eta} = 2\pi\eta E^{1/2} = \pi(2m)^{1/2} \frac{Z_j Z_k e^2}{\hbar} \,. \tag{18.25}$$

A further evaluation of $\langle \sigma v \rangle$ requires a specification of $S(E)$. We shall limit ourselves to the simplest but for astrophysical applications very important case of *non-resonant reactions*. Then we can set $S(E) \approx S_0 =$ constant, and take it out of the integral (18.24), since only a small interval of E will turn out to contribute appreciably. The remaining integral may be written as

$$J = \int_0^\infty \mathrm{e}^{f(E)} dE \,, \quad \text{with} \quad f(E) = -\frac{E}{kT} - \frac{\bar{\eta}}{E^{1/2}} \,. \tag{18.26}$$

The integrand is the product of two exponential functions, one of which drops steeply with increasing E, while the other rises. The integrand will therefore have appreciable values only around a well-defined maximum (see Fig. 18.5), the so-called *Gamow peak*. This maximum occurs at E_0, where the exponent has a minimum. From the condition $f' = 0$, where f' is the derivative with respect to E, one finds

$$E_0 = \left(\frac{1}{2}\bar{\eta} kT\right)^{2/3} = \left[\left(\frac{m}{2}\right)^{1/2} \pi \frac{Z_i Z_k e^2 kT}{\hbar}\right]^{2/3} \,. \tag{18.27}$$

It is usual to introduce now a quantity τ defined by

$$\tau = 3\frac{E_0}{kT} = 3\left[\pi\left(\frac{m}{2kT}\right)^{1/2}\frac{Z_j Z_k e^2}{\hbar}\right]^{2/3} \tag{18.28}$$

and to represent $f(E)$ near the maximum by the series expansion

$$\begin{aligned} f(E) &= f_0 + f_0' \cdot (E - E_0) + \frac{1}{2} f_0'' \cdot (E - E_0)^2 + \cdots \\ &= -\tau - \frac{1}{4}\tau\left(\frac{E}{E_0} - 1\right)^2 + \cdots , \end{aligned} \tag{18.29}$$

from which we retain only these two terms (the linear term vanishes since $f_0' = 0$ at the maximum). Their substitution in (18.26) means to approximate the Gamow peak of the integrand by a Gaussian, as will become particularly clear when we transform J to the new variable of integration $\xi = (E/E_0 - 1)\sqrt{\tau}/2$:

$$J = \int_0^\infty \exp\left[-\tau - \frac{\tau}{4}\left(\frac{E}{E_0} - 1\right)^2\right] dE = \frac{2}{3} kT\tau^{1/2} \mathrm{e}^{-\tau} \int_{-\sqrt{\tau/2}}^\infty \mathrm{e}^{-\xi^2} d\xi \ . \tag{18.30}$$

The main contribution to J comes from a range close to $E = E_0$, i.e. $\xi = 0$, so that no large errors are introduced when extending the range of integration to $-\infty$, the integral over the Gaussian becoming $\sqrt{\pi}$.

We then have

$$J \approx kT\frac{2}{3}\pi^{1/2}\tau^{1/2}\mathrm{e}^{-\tau} \ , \tag{18.31}$$

and for non-resonant reactions (18.24) becomes

$$\langle \sigma v \rangle = \frac{4}{3}\left(\frac{2}{m}\right)^{1/2} \frac{1}{(kT)^{1/2}} S_0 \tau^{1/2} \mathrm{e}^{-\tau} \ . \tag{18.32}$$

From (18.28) one has $(kT)^{-1/2} \sim \tau^{3/2}$; hence the kT can be substituted in (18.32), which then gives $\langle \sigma v \rangle \sim \tau^2 \mathrm{e}^{-\tau}$.

The *properties of the Gamow peak* are so important that we should inspect some of them a bit further. In order to have convenient numerical values, we count the temperature in units of 10^7 K (which is typical for many stellar centres) and denote this dimensionless temperature by $T_7 = T/10^7$ K or generally

$$T_n := \frac{T}{10^n \text{ K}} \ . \tag{18.33}$$

We then have the following relations (some of which will be derived below):

$$
\begin{aligned}
W &= Z_j^2 Z_k^2 A = Z_j^2 Z_k^2 \frac{A_j A_k}{A_j + A_k} \,, \\
\tau &= 19.721 W^{1/3} T_7^{-1/3} \,, \\
E_0 &= 5.665\,\mathrm{keV} \cdot W^{1/3} T_7^{2/3} \,, \\
\frac{E_0}{kT} &= \frac{\tau}{3} = 6.574 W^{1/3} T_7^{-1/3} \,, \\
\Delta E &= 4.249\,\mathrm{keV} \cdot W^{1/6} T_7^{5/6} \,, \\
\frac{\Delta E}{E_0} &= 4(\ln 2)^{1/2} \tau^{-1/2} = 0.750 W^{-1/6} T_7^{1/6} \,, \\
\nu &= \partial \ln\langle \sigma v \rangle / \partial \ln T = (\tau - 2)/3 = 6.574 W^{1/3} T_7^{-1/3} - 2/3 \,. \qquad (18.34)
\end{aligned}
$$

The value of W is determined by the reaction partners and is at least of order unity. Large W discriminates against the reactions of heavy nuclei so much that only the lighter nuclei can react with appreciable rate. The Gamow peak occurs as a compromise in the counteraction between Maxwell distribution and penetration probability with a maximum at $E = E_0$, which is roughly 5–100 times the average thermal energy kT. This "effective stellar energy range" is, on the other hand, far below the $\gtrsim$100 keV available to most laboratory experiments. With increasing T, E_0 increases moderately, while the maximum height of the peak $H_0 = \mathrm{e}^{-\tau}$ increases very steeply owing to the decreasing τ.

The width of the effective energy range is described by ΔE, which is the full width of the Gamow peak at half maximum (see Fig. 18.5), i.e. between the points with height 0.5 $\mathrm{e}^{-\tau}$. Equating this to the integrand in the first form of (18.30), we obtain

$$
\frac{\Delta E}{E_0} = 4 \frac{(\ln 2)^{1/2}}{\tau^{1/2}} \,. \qquad (18.35)
$$

According to (18.34), this is always below unity, and therefore one has a well-defined energy range in which the reactions occur effectively. With ΔE increasing with T only slightly more than E_0, the relative form of the peak remains nearly constant.

The most striking feature of thermonuclear reactions is their strong sensitivity to the temperature. In order to demonstrate this, one represents the T dependence of $\langle \sigma v \rangle$ (and thus of r_{jk} and ε_{jk}) around some value $T = T_0$ by a power law such as

$$
\langle \sigma v \rangle = \langle \sigma v \rangle_0 \left(\frac{T}{T_0} \right)^{\nu} \,, \quad \nu = \frac{\partial \ln \langle \sigma v \rangle}{\partial \ln T} \,. \qquad (18.36)
$$

From (18.28) we have $\tau \sim T^{-1/3}$, and then from (18.32) $\langle \sigma v \rangle \sim T^{-2/3} \mathrm{e}^{-\tau}$. Therefore

$$\ln\langle \sigma v \rangle = \text{constant} - \frac{2}{3} \ln T - \tau \ , \tag{18.37}$$

and

$$\frac{\partial \ln\langle \sigma v \rangle}{\partial \ln T} = -\frac{2}{3} - \frac{\partial \tau}{\partial \ln T} = -\frac{2}{3} - \tau \frac{\partial \ln \tau}{\partial \ln T} \ . \tag{18.38}$$

Since $\tau \sim T^{-1/3}$, we have $\partial \ln \tau / \partial \ln T = -1/3$, so that finally

$$\nu \equiv \frac{\partial \ln\langle \sigma v \rangle}{\partial \ln T} = \frac{\tau}{3} - \frac{2}{3} \ , \tag{18.39}$$

where for most reactions $\tau/3$ is much larger than 2/3 and $\nu \approx \tau/3$. Then ν decreases with T as $\nu \sim T^{-1/3}$. From (18.34) we see that even for reactions between the lightest nuclei, $\nu \approx 5$, and it can easily attain values around (and even above) $\nu \approx 20$. With such values for the exponent (!) of T, the thermonuclear reaction rate is about the most strongly varying function treated in physics, and this temperature sensitivity has a clear influence on stellar models. Also, since small fluctuations of T (which will certainly be present) must result in drastic changes in the energy production, we have to assume that there exists an effective stabilizing mechanism (a thermostat) in stars (Sect. 25.3.5).

We may easily see how the large ν values are related to the change of the Gamow peak with T: the value $\langle \sigma v \rangle$ is proportional to the integral J in (18.30), and this is given by the area under the Gamow peak, which is roughly $J \approx \Delta E \cdot H_0 (H_0 = \mathrm{e}^{-\tau}$ is the height of the peak). According to (18.34), $\Delta E \sim T^{5/6}$, while H_0 increases strongly with T. In fact it is this height H_0 which provides the exponential $\mathrm{e}^{-\tau}$ in the expressions for $\langle \sigma v \rangle$ and is therefore responsible for the large values of ν.

We should briefly mention a few corrections to the derived formulae for the reaction rates. The first concerns inaccuracies made by evaluating the integral in (18.24) with constant S and with an integrand approximated by a Gaussian. This is usually corrected for by multiplying $\langle \sigma v \rangle$ with a factor

$$g_{jk} = 1 + \frac{5}{12\tau} + \frac{S'}{S} E_0 \left(1 + \frac{105}{36\tau} \right) + \frac{1}{2} \frac{S''}{S} E_0^2 \left(1 + \frac{267}{36\tau} \right) \ , \tag{18.40}$$

where S and its derivatives with respect to E have to be taken at $E = 0$ (Eq. (17.206b) in Weiss et al. 2004, p. 601).

Another correction factor, f_{jk}, allows for a partial shielding of the Coulomb potential of the nuclei, owing to the negative field of neighbouring electrons. This plays a role only at very high densities; it will be treated separately in Sect. 18.4.

Concerning resonant reactions we shall only remark that the situation depends very much on the location of the resonance. For example, the integral in (18.24) can be dominated by a strong peak at the resonance energy. However, once $S(E)$ is given, (18.24) can in principle always be evaluated.

18.4 Electron Shielding

We have seen that the repulsive Coulomb forces of the nucleus play a decisive role in controlling the rate of thermonuclear reactions. Therefore any modification of its potential by influences from the outside can have an appreciable effect on these rates. An obvious effect to be considered comes from the surrounding free electrons. It is clear that beyond a certain distance an approaching particle will "feel" a neutral conglomerate of the target nucleus plus a surrounding electron cloud rather than the isolated charge of the target nucleus.

The first step is to consider the polarization that the nucleus of charge $+Ze$ produces in its surrounding. The electrons of charge $-e$ are attracted and have a slightly larger density n_e in the neighbourhood of the nucleus; the other ions are repelled and have a slightly decreased density n_i in comparison with their average values $\bar{n}_\mathrm{e}$ and $\bar{n}_i$ (without electric fields present). For non-degenerate gases the density of particles with charge q is modified in the presence of an electrostatic potential ϕ according to

$$n = \bar{n}\mathrm{e}^{-q\phi/kT} \,. \tag{18.41}$$

In most normal cases one will find $|q\phi| \ll kT$ and can then approximate the exponential by $1 - q\phi/kT$. For ions and electrons, (18.41) now yields

$$n_i = \bar{n}_i \left(1 - \frac{Z_i e\phi}{kT}\right) \,, \quad n_\mathrm{e} = \bar{n}_\mathrm{e} \left(1 + \frac{e\phi}{kT}\right) \,, \tag{18.42}$$

which shows directly the decrease (ions) and increase (electrons) of the two densities.

Considering the n_i for all types of ions present in the gas mixture, one can immediately write down the total charge density σ. For $\phi = 0$ one must have a neutral gas, with $\bar{\sigma} = 0$, i.e.

$$\bar{\sigma} = \sum_i (Z_i e)\bar{n}_i - e\bar{n}_\mathrm{e} = 0 \,, \tag{18.43}$$

whereas for non-vanishing ϕ we have

$$\begin{aligned} \sigma &= \sum_i (Z_i e) n_i - e n_\mathrm{e} \\ &= \sum_i -\frac{(Z_i e)^2 \phi}{kT} \bar{n}_i - \frac{e^2\phi}{kT} \bar{n}_\mathrm{e} \,. \end{aligned} \tag{18.44}$$

Here we have already inserted (18.42) and made use of (18.43) to eliminate the ϕ-independent terms. The second expression (18.44) suggests that we combine the two terms and write

$$\sigma = -\chi \frac{e^2 \phi}{kT} n \ , \tag{18.45}$$

where we have introduced the total particle density $n = n_\mathrm{e} + \sum_i n_i$ and the average value χ:

$$\chi := \frac{1}{n} \left(\sum_i Z_i^2 \bar{n}_i + \bar{n}_\mathrm{e} \right) \ . \tag{18.46}$$

If one wishes to use the mass fraction $X_i = A_i \bar{n}_i / n\mu$ (μ = mean molecular weight per free particle, see Sect. 4.2, (4.27)) instead of the particle numbers, the expression follows simply as

$$\chi = \mu \zeta = \mu \sum_i \frac{Z_i (Z_i + 1)}{A_i} X_i \ . \tag{18.47}$$

The charge density σ and the electrostatic potential ϕ are also connected by the Poisson equation

$$\nabla^2 \phi = -4\pi\sigma \ . \tag{18.48}$$

If we assume spherical symmetry for the charge distribution surrounding the nucleus under consideration, the Laplace operator ∇^2 then reduces to its well-known radial part. Introducing σ from (18.45) on the right-hand side of (18.48), the Poisson equation becomes

$$\frac{r_\mathrm{D}^2}{r} \frac{d^2(r\phi)}{dr^2} = \phi \ , \tag{18.49}$$

where we have scaled the distance r by the so-called Debye–Hückel length

$$r_\mathrm{D} = \left(\frac{kT}{4\pi\chi e^2 n} \right)^{1/2} \ . \tag{18.50}$$

One readily verifies that (18.49) is solved by

$$\phi = \frac{Ze}{r} \mathrm{e}^{-r/r_\mathrm{D}} \ , \tag{18.51}$$

and this shows that ϕ tends to the normal (unshielded) potential Ze/r of a point charge Ze for small distances, $r \to 0$, while we have an essential reduction of this "normal" potential at distances $r \gtrsim r_\mathrm{D}$. In a certain sense we can call r_D the "radius" of the electron cloud that envelopes the nucleus and shields part of its potential for an outside viewer.

The values of ζ in (18.47) are of order unity. For $T = 10^7\,\mathrm{K}$ and ϱ between 1 and $10^2\,\mathrm{g\,cm^{-3}}$, r_D has typical values of $10^{-8} \cdots 10^{-9}\,\mathrm{cm}$. In order to judge the influence of the shielding on nuclear reactions between nuclei of types 1 and 2, we should compare r_D with the closest distance r_{c0} to which the particles can classically approach each other if their energy is that of the Gamow peak E_0 [given by (18.27)]. These particles will be the most effective ones for the energy production. According

to (18.7) one has $r_{c0} = Z_1 Z_2 e^2/E_0$, and convenient numerical expressions for E_0 are given in (18.34). We then find

$$\frac{r_D}{r_{c0}} \approx 200 \frac{E_0}{Z_1 Z_2} \left(\frac{T_7}{\zeta \varrho}\right)^{1/2} , \tag{18.52}$$

where E_0 is in keV and ϱ in g cm^{-3}. With rough values for the solar centre, $T_7 \approx 1$, $\varrho \approx 10^2$ g cm^{-3}, $\zeta \approx 1$, and for the most important hydrogen reactions, we have $Z_1 Z_2 = 1 \ldots 7$ and $E_0 \approx 5 \ldots 20$ keV; hence (18.52) gives $r_D/r_{c0} \approx 50 \ldots 100$. For all such "normal" stars, $r_D \gg r_{c0}$, which means that the incoming particle even classically (without the tunnelling effect) penetrates nearly the entire electron cloud and the shielding will have little effect at these critical distances.

The decrease of the Coulomb interaction energy E_{Coul} increases the probability P_0 for tunnelling through the Coulomb wall. The decisive exponent η in P_0 [(18.9) and the following] is determined by the function $E_{Coul} - E$. The energy E_{Coul} is now reduced according to (18.51) by the factor $\exp(-r/r_D)$, which is to a first approximation $1 - r/r_D$ for $r/r_D \ll 1$.

This gives

$$E_{Coul} - E \equiv \frac{Z_1 Z_2 e^2}{r} e^{-r/r_D} - E \approx \frac{Z_1 Z_2 e^2}{r} - \frac{Z_1 Z_2 e^2}{r_D} - E , \tag{18.53}$$

which shows that we will obtain the same result as without shielding, but with an enlarged energy:

$$\tilde{E} = E + \frac{Z_1 Z_2 e^2}{r_D} = E + E_D . \tag{18.54}$$

In order to see the influence on simple non-resonant reaction rates, consider the integrand in (18.21) and replace $\sigma(E)$ by $\sigma(\tilde{E})$. With (18.15) and (18.19) and $\tilde{\eta} = \eta (E/\tilde{E})^{1/2}$, we have the proportionality

$$\begin{aligned} \sigma(\tilde{E}) v f(E) &\sim (\tilde{E}^{-1} e^{-2\pi\tilde{\eta}}) E^{1/2} (E^{1/2} e^{-E/kT}) \\ &\sim \left(1 - \frac{E_D}{\tilde{E}}\right) e^{E_D/kT - \tilde{E}/kT - 2\pi\tilde{\eta}} . \end{aligned} \tag{18.55}$$

We assume here that $E_D/kT \ll 1$, which is usually called the case of "weak screening". Considering the fact that only a small range of E at values much larger than kT contributes essentially to $\langle \sigma v \rangle$, we may as well neglect the factor $(1 - E_D/\tilde{E})$ in (18.55) and integrate over $\tilde{E}$ instead of E. The main change is then the additional constant exponent E_D/kT such that $\langle \sigma v \rangle$ is multiplied by a "screening factor"

$$f = e^{E_D/kT} , \tag{18.56}$$

which increases $\langle \sigma v \rangle$, since E_D is positive. For weak screening we have numerically

$$\frac{E_D}{kT} = \frac{Z_1 Z_2 e^2}{r_D kT} = 5.92 \times 10^{-3} Z_1 Z_2 \left(\frac{\zeta \varrho}{T_7^3} \right)^{1/2} , \tag{18.57}$$

with ϱ in g cm^{-3}. For $\zeta \approx 1, \varrho = 1$ g cm^{-3}, and $T_7 = 1$, reactions with $Z_1 Z_2 \lesssim 16$ require correction factors f, which increase the rate by less than 10 %.

Where very large densities are involved, however, one will leave the regime of weak screening. For $E_D/kT \gtrsim 1$, the treatment is much more complicated, and the limiting case of "strong screening" is described approximately by

$$\frac{E_D}{kT} \approx 0.0205[(Z_1 + Z_2)^{5/3} - Z_1^{5/3} - Z_2^{5/3}] \frac{(\varrho/\mu_e)^{1/3}}{T_7} , \tag{18.58}$$

with the molecular weight per free electron $\mu_e = (\sum X_i Z_i / A_i)^{-1}$, see (4.29), and ϱ in g cm^{-3}.

Equations (18.57) and (18.58) show that the screening factor f increases appreciably for increasing ϱ and decreasing T. While f was a minor correction factor to the rate for "normal" stars with weak screening, the situation changes completely in the high-density, low-temperature regime, where screening becomes the dominating factor in the reaction rate.

Consider the shielded reaction rate as represented by

$$f \langle \sigma v \rangle = f_0 \langle \sigma v \rangle_0 \left(\frac{\varrho}{\varrho_0} \right)^{\lambda} \left(\frac{T}{T_0} \right)^{\nu} \tag{18.59}$$

in the neighbourhood of ϱ_0, T_0. In a similar manner to the derivation of ν for the unshielded case in (18.36)–(18.39), we find now that

$$\nu = \frac{\tau}{2} - \frac{2}{3} - \frac{E_D}{kT} ; \quad \lambda = 1 + \frac{1}{3} \frac{E_D}{kT} . \tag{18.60}$$

For very high densities and moderate to low temperatures (say $\varrho > 10^6$ g cm^{-3}, $T > 10^7$ K), the temperature sensitivity ν decreases, while the density sensitivity λ becomes larger. This can be seen from Fig. 18.6, where the line of constant ^{12}C–^{12}C burning turns steeply down for large ϱ. Finally, the reaction rates now depend mainly on the density (instead of the temperature) and one speaks of *"pycnonuclear reactions"*. For ^{12}C burning in a pure ^{12}C plasma, (18.60) gives the transition $\lambda = \nu$ at $T_7 = 10$ for $\varrho = 1.60 \times 10^9$ g cm^{-3}.

Pycnonuclear reactions can play a role in very late phases of stellar evolution, where a burning may be triggered by a compression without temperature increase, and they can provide a certain amount of energy release even in cool stars, if only the density is high enough. Of course, other effects, such as the decrease of the mobility of the nuclei because of crystallization, must then also be considered.

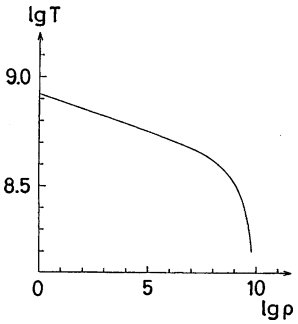

Fig. 18.6 A line of constant energy generation rate $\varepsilon(=10^4\ \mathrm{erg\,g^{-1}\,s^{-1}})$ for the $^{12}C+^{12}C$ burning in a diagram showing the temperature T (in K) over the density ϱ (in $\mathrm{g\,cm^{-3}}$). The temperature sensitivity ν and the density sensitivity λ are equal where the slope is -1

18.5 The Major Nuclear Burning Stages

Although no chemical reactions are involved, one usually calls the thermonuclear fusion of a certain element the "burning" of this element. Owing to the properties of thermonuclear reaction rates, different burnings are well separated by appreciable temperature differences. A review of the cross sections for all possible reactions in the major burning stages shows that only very few reactions occur with non-negligible rates during a certain phase. The most important ones will be listed below. Their important properties, such as the astrophysical factors S_0, correction factors to (18.32), or energy release Q, can be found in the literature (e.g. Caughlan and Fowler 1988; Harris and Fowler 1983; Adelberger et al. 2011; Angulo et al. 1999).

The Q values usually contain all of the energy made available to the stellar matter by one such reaction. This includes the energies of the γ rays that are either directly emitted or created by pair annihilation after e^+ emission. Excluded, however, is the energy carried away by neutrinos, since they normally do not interact with the stellar material.

A whole "network" of all simultaneously occurring reactions (8.7) has to be calculated if one is interested in details such as the isotopic abundances produced by the reactions or if the star changes on a timescale comparable with that of one of the reactions. The total ε is then obtained as a sum of (18.23) over all reactions, and one has to ensure the correct bookkeeping of the changing abundances of all nuclei involved. We have encountered nuclear reaction networks also in Sect. 12.3.

If one is interested only in the energy production, often, a much simpler procedure suffices in which only the rate for the slowest of a chain of subsequent reactions is calculated, since it determines essentially the rate of the whole fusion process. An example of such a "bottleneck" is the ^{14}N reaction in the CNO cycle (see below). Then (18.23) has to be used for this reaction, but with Q equal to the sum of all energies released in the single reactions.

In this section, all formulae for ε will be given in units of $\mathrm{erg\,g^{-1}s^{-1}}$, ϱ in $\mathrm{g\,cm^{-3}}$, and T in the dimensionless form $T_n = T/10^n$ K. As usual we denote by X_j the mass fraction of nuclei with mass number $A = j$.

18.5.1 Hydrogen Burning

The net result of hydrogen burning is the fusion of four ^{1}H nuclei into one ^{4}He nucleus. The difference in binding energy is almost exactly 27.0 MeV, corresponding to a mass defect of about 0.7 per cent. This is roughly 10 times the energy liberated in any other fusion process, though not all of this energy is available to stellar matter. The fusion requires the transformation of two protons into neutrons, i.e. two β^+ decays, which must be accompanied by two neutrino emissions (conservation of lepton number). The neutrinos carry away 2 . . . 30 per cent of the whole energy liberated, the amount depending strongly on the reaction in which they are emitted.

There are different chains of reactions by which a fusion process can be completed and which in general will occur simultaneously in a star. The two main series of reactions are known as the proton–proton chain and the CNO cycle.

The *proton–proton chain* (*pp* chain) is named after its first reaction, between two protons forming a deuterium nucleus ^{2}H, which then reacts with another proton to form ^{3}He:

$$\begin{aligned} {}^1\mathrm{H} + {}^1\mathrm{H} &\rightarrow {}^2\mathrm{H} + e^+ + \nu \,, \\ {}^2\mathrm{H} + {}^1\mathrm{H} &\rightarrow {}^3\mathrm{He} + \gamma \,. \end{aligned} \tag{18.61}$$

The first of these reactions is unusual in comparison with most other fusion processes. In order to form ^{2}H, the protons have to experience a β^+ decay at the time of their closest approach. This is a process governed by the weak interaction and is very unlikely. Therefore the first reaction has a very small cross section.

The completion of a ^{4}He nucleus can proceed via one of three alternative branches (*pp*1, *pp*2, *pp*3) all of which start with ^{3}He. The first alternative requires two ^{3}He nuclei, i.e. the reactions in (18.61) have first to be completed twice. The other alternatives require that ^{4}He already exists (either it is present because of its primordial abundance, or because it was already produced earlier by this burning process). The branching between *pp*2 and *pp*3 exists, since ^{7}Be can react either with e^- or with ^{1}H. All possibilities can be seen from the following scheme:

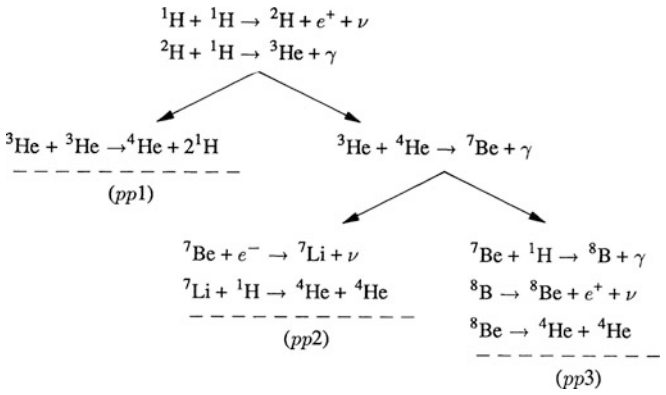

(18.62)

Owing to the different energies carried away by the neutrinos, the energies released to the stellar matter differ for the three chains. They are $Q = 26.50(pp1)$, $25.97(pp2)$, and $19.59(pp3)$, in MeV per produced ^{4}He nucleus. For each quantity Q released, the first two reactions of (18.61) have to be performed only once in the $pp2$ and $pp3$ branches.

Three reactions in (18.62) release neutrinos, which are given names according to the element being processed in these reactions: pp-, ^{7}Be-, and ^{8}B-neutrinos. If they are the only lepton emitted, then their energy is well defined. The ^{7}Be-neutrinos carry away 0.863 MeV in 90 % of the reactions, and 0.386 MeV in the remaining 10 %, depending on the energy state of ^{7}Li produced. If the neutrinos are emitted along with a positron (e^+), the two leptons share the energy, and a spectrum of neutrino energies results. The upper limits are 0.423 MeV for the pp-neutrinos and 15 MeV for those of the ^{8}B reaction. The average values are 0.267 and 6.735 MeV respectively.

The relative frequency of the different branches depends on the chemical composition, the temperature, and the density. The ^{3}He–^{4}He reaction has a 14 % larger reduced mass, a 4.6 % larger τ, and thus a slightly larger temperature sensitivity ν than the ^{3}He–^{3}He reaction, cf. (18.34) and (18.39). With increasing T, $pp2$ and $pp3$ will therefore dominate more and more over $pp1$ (say above $T_7 \approx 1$) if ^{4}He is present in appreciable amounts. And with increasing T, the relative importance will gradually shift from the electron capture ($pp2$) to the proton capture ($pp3$) of ^{7}Be.

The energy generation in the pp chain should be calculated at small T (say below $T_6 \approx 8$) by calculating all single reactions and their influence on the nuclei involved. For larger T, there will be an equilibrium abundance established for these nuclei (equal rates of consumption and production) and one can simply take the whole ε_{pp} as proportional to that of the $pp1$ branch, which in turn may be calculated from the rate of the first reaction $^1\mathrm{H} + {}^1\mathrm{H}$:

$$\begin{aligned} \varepsilon_{pp} &= 2.57 \times 10^4 \psi f_{11} g_{11} \varrho X_1^2 T_9^{-2/3} \mathrm{e}^{-3.381/T_9^{1/3}} \,, \\ g_{11} &= (1 + 3.82T_9 + 1.51T_9^2 + 0.144T_9^3 - 0.0114T_9^4) \,, \end{aligned} \tag{18.63}$$

where ε_{pp} and ϱ are in cgs and f_{11} is the shielding factor for this reaction. The factor ψ corrects for the additional energy generation in the branches $pp2$ and $pp3$ if there is appreciable ^{4}He present (see Fig. 18.7). For gradually increasing T, ψ starts with the value 1 and can then increase to values close to 2 (at $T_7 \approx 2$), at which point $pp2$ takes over, since then *each* ^{1}H–^{1}H reaction gives one ^{4}He (compared to *every second* such reaction in the branch $pp1$). After this maximum, ψ decreases again to about 1.5 where $pp3$ has taken over owing to its Q being much smaller than those of the other branches.

The formulation of the energy generation ε as given in (18.63) is an analytical fit to measured and tabulated values, based on T-dependences of non-resonant reactions and resonances. They may vary from group to group; the one used here is taken from Angulo et al. (1999).

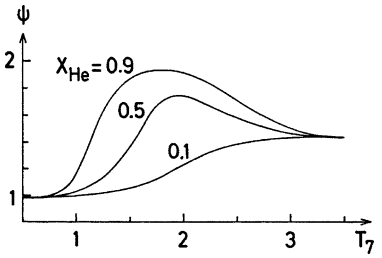

Fig. 18.7 The correction ψ for ε_{pp} as a function of T_7, for three different helium abundances (After Parker et al. 1964)

The temperature sensitivity of the *pp* chain is the smallest of all fusions. At $T_6 = 5$, we have $\nu \approx 6$, which decreases to 3.5 at $T_6 \approx 20$.

The *CNO cycle* is the other main series of reactions in hydrogen burning. It requires the presence of some isotopes of C, N, or O, which are reproduced in a manner similar to catalysts in chemical reactions. The sequence of reactions can be represented as follows:

$$
\begin{aligned}
&{}^{12}\mathrm{C} + {}^{1}\mathrm{H} \rightarrow {}^{13}\mathrm{N} + \gamma \\
&{}^{13}\mathrm{N} \rightarrow {}^{13}\mathrm{C} + e^{+} + \nu \\
&{}^{13}\mathrm{C} + {}^{1}\mathrm{H} \rightarrow {}^{14}\mathrm{N} + \gamma \\
&{}^{14}\mathrm{N} + {}^{1}\mathrm{H} \rightarrow {}^{15}\mathrm{O} + \gamma \\
&{}^{15}\mathrm{O} \rightarrow {}^{15}\mathrm{N} + e^{+} + \nu \\
&{}^{15}\mathrm{N} + {}^{1}\mathrm{H} \rightarrow {}^{12}\mathrm{C} + {}^{4}\mathrm{He} \\
&\qquad\qquad\quad \rightarrow {}^{16}\mathrm{O} + \gamma \\
&{}^{16}\mathrm{O} + {}^{1}\mathrm{H} \rightarrow {}^{17}\mathrm{F} + \gamma \\
&{}^{17}\mathrm{F} \rightarrow {}^{17}\mathrm{O} + e^{+} + \nu \\
&{}^{17}\mathrm{O} + {}^{1}\mathrm{H} \rightarrow {}^{14}\mathrm{N} + {}^{4}\mathrm{He}
\end{aligned}
\tag{18.64}
$$

The main cycle (CNO-I; upper 6 lines of this scheme) is completed after the initially consumed ^{12}C is reproduced by $^{15}\mathrm{N} + {}^{1}\mathrm{H}$. This reaction shows a branching via ^{16}O into a secondary cycle (CNO-II; connected with the main cycle by dashed arrows), which is, however, roughly 10^3 times less probable. Its main effect is that the ^{16}O nuclei originally present in the stellar matter can also take part in the cycle, since they are finally transformed into ^{14}N by the last three reactions of (18.64). The decay times for the β^+ decays are of the order of $10^2 \ldots 10^3$ s. As usual, a network of all simultaneous reactions has to be calculated for lower temperatures, rapid changes, or if a detailed knowledge about the abundances of all nuclei involved is desired.

As in the case of the *pp* chains, two protons have to be converted in effect to neutrons in the process, which will release two neutrinos per new helium nucleus.

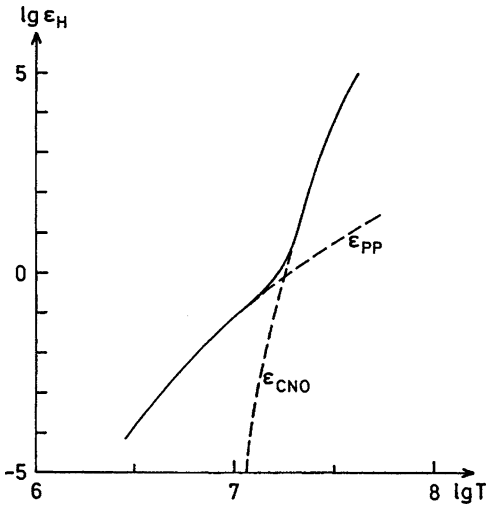

Fig. 18.8 Total energy generation rate $\varepsilon_{\rm H}$ (in erg g^{-1} s^{-1}) for hydrogen burning (*solid line*) over the temperature T (in K), for $\varrho = 1\,{\rm g\,cm^{-3}}$, $X_1 = 1$, and $X_{\rm CNO} = 0.01$. The contributions of the *pp* chain and the CNO cycle are *dashed*

The ^{13}N-, ^{15}O-, and ^{17}F-neutrinos of the CNO-cycles have all energy spectra with an upper limit between 1.1 and 1.7 MeV, and an average energy of 0.706, 0.996, and 0.998 MeV.

Most stars change slowly enough that, for sufficiently high temperature (say $T_7 \gtrsim 1.5$), the nuclei involved in the cycle reach their equilibrium abundance (i.e. the rate of production equals that of consumption). Then it suffices to calculate explicitly only the slowest reaction, which is $^{14}{\rm N}+^{1}{\rm H}$ and which essentially controls the time for completing the cycle. $\varepsilon_{\rm CNO}$ will then be given by the rate of this reaction and by the energy gain of the whole cycle, which is 24.97 MeV. This slowest reaction acts like a bottleneck where the nuclei involved are congested in their "flow" through the cycle. Nearly all of the initially present C, N, and O nuclei will therefore be found as ^{14}N, waiting to be transformed to ^{15}O. The energy generation rate can be written as (using again the cross section from Angulo et al. 1999 but dropping additional terms important for higher temperatures for simplicity)

$$\begin{aligned} \varepsilon_{\rm CNO} &= 8.24\times 10^{25} g_{14,1} X_{\rm CNO} X_1 \varrho T_9^{-2/3} {\rm e}^{(-15.231 T_9^{-1/3} - (T_9/0.8)^2)} \,, \\ g_{14,1} &= (1 - 2.00 T_9 + 3.41 T_9^2 - 2.43 T_9^3) \,, \end{aligned} \tag{18.65}$$

where $\varepsilon_{\rm CNO}$ and ϱ are in cgs. $X_{\rm CNO}$ is the sum of $X_{\rm C}$, $X_{\rm N}$, and $X_{\rm O}$. The temperature sensitivity ν is much higher here than in the *pp* chain. For $T_6 = 10 \ldots 50$, we find $\nu \approx 23 \ldots 13$. This has the consequence that the *pp* chain dominates at low temperatures ($T_6 < 15$), while it can be neglected against $\varepsilon_{\rm CNO}$ for higher temperatures (see Fig. 18.8). Hydrogen burning normally occurs in the range $T_6 \approx 8 \ldots 50$, since at larger T, the hydrogen is very rapidly exhausted.

18.5.2 Helium Burning

The reactions of helium burning consist of the gradual fusion of several ^{4}He into ^{12}C, ^{16}O, ... This requires temperatures of $T_8 \gtrsim 1$, i.e. appreciably higher than those for hydrogen burning, because of the higher Coulomb barriers.

The first and key reaction is the formation of ^{12}C from three ^{4}He nuclei, which is called the *triple α reaction* (or 3α reaction). A closer look shows that it is performed in two steps, since a triple encounter is too improbable:

$$\begin{aligned} {}^4\mathrm{He} + {}^4\mathrm{He} &\rightleftarrows {}^8\mathrm{Be} \,, \\ {}^8\mathrm{Be} + {}^4\mathrm{He} &\rightarrow {}^{12}\mathrm{C} + \gamma \,. \end{aligned} \tag{18.66}$$

In the first step, two α particles temporarily form a ^{8}Be nucleus. Its ground state is nearly 100 keV higher in energy and therefore decays back into the two α's after a few times 10^{-16} s. This seems to be a very short time at a first glance, but it is roughly 10^5 times larger than the duration of a normal scattering encounter. The probability for another reaction occurring during this time is correspondingly enhanced. In fact the lifetime of ^{8}Be is sufficient to build up an average concentration of these nuclei of about 10^{-9} in the stellar matter. The high densities then ensure a sufficient rate of further α captures that form ^{12}C nuclei [the second step in (18.66)]. Both these reactions are complicated owing to the involvement of resonances. The energy release per ^{12}C nucleus formed is 7.274 MeV. This gives an energy release *per unit mass* that is 10.4 times smaller than in the case of the CNO cycle (where only four instead of 12 nucleons are processed): $E_{3\alpha} = 5.8 \times 10^{17}\,\mathrm{erg\,g^{-1}}$. The resulting energy generation rate is

$$\varepsilon_{3\alpha} = 5.09 \times 10^{11}\, f_{3\alpha}\, \varrho^2 X_4^3 T_8^{-3} \mathrm{e}^{-44.027/T_8} \tag{18.67}$$

(ε and ϱ in cgs), with the screening factor $f_{3\alpha}$. (18.67) is based on an older, simplified analytical fit of $\langle \sigma v \rangle$ by Caughlan and Fowler (1988). A more recent one, taken from the compilation by Angulo et al. (1999), has more terms, reflecting the effect of the several resonances involved:

$$\begin{aligned} \varepsilon_{3\alpha} = {} & 6.272 \varrho^2 X_4^3 \cdot (1 + 0.0158 T_9^{-0.65}) \\ & \times \Big[2.43 \times 10^9 T_9^{-2/3} \exp\left(-13.490 T_9^{-1/3} - (T_9/0.15)^2 \right) \cdot (1 + 74.5 T_9) \\ & \quad + 6.09 \times 10^5 T_9^{-3/2} \exp(-1.054/T_9) \Big] \\ & \times \Big[2.76 \times 10^7 T_9^{-2/3} \exp\left(-23.570 T_9^{-1/3} - (T_9/0.4)^2 \right) \\ & \quad \times (1 + 5.47 T_9 + 326 T_9^2) + 130.7 T_9^{-3/2} \exp(-3.338/T_9) \\ & \quad + 2.51 \times 10^4 T_9^{-3/2} \exp(-20.307/T_9) \Big] \,. \end{aligned} \tag{18.68}$$

The two terms in square brackets in (18.68) come from the $\alpha + \alpha$ and the $\alpha + {}^{8}$Be steps of the 3α-process; the first line contains also a conversion factor to go from the mean cross section to the energy production rate according to (18.23). This reaction has an enormous temperature sensitivity. For $T_8 = 1 \ldots 2$, (18.39) gives $\nu \approx 40 \ldots 19$!

Once a sufficient ^{12}C abundance has been built up by the 3α reaction, further α captures can occur simultaneously with (18.66) such that the nuclei ^{16}O, ^{20}Ne, ... are successively formed:

$$\begin{aligned} {}^{12}\mathrm{C} \; + \; {}^{4}\mathrm{He} &\rightarrow {}^{16}\mathrm{O} + \gamma \; , \\ {}^{16}\mathrm{O} \; + \; {}^{4}\mathrm{He} &\rightarrow {}^{20}\mathrm{Ne} + \gamma \; , \\ &\ldots \end{aligned} \tag{18.69}$$

In a typical stellar-interior environment, reactions going beyond ^{20}Ne are rare.

The energy release per $^{12}\mathrm{C}(\alpha,\gamma)^{16}\mathrm{O}$ reaction is 7.162 MeV, corresponding to $E_{12,\alpha} = 4.320 \times 10^{17}\,\mathrm{erg\,g^{-1}}$ of produced ^{16}O (The whole formation of ^{16}O from the initial four α particles has then yielded $8.71 \times 10^{17}\,\mathrm{erg\,g^{-1}}$.). This is a rather complicated reaction. For moderate temperatures (up to a few 10^8 K), one may use the following simple approximation:

$$\varepsilon_{12,\alpha} = 1.3 \times 10^{27} f_{12,4} X_{12} X_4 \varrho T_8^{-2} \left(\frac{1 + 0.134 T_8^{2/3}}{1 + 0.017 T_8^{2/3}} \right)^2 \mathrm{e}^{-69.20/T_8^{1/3}} \; , \tag{18.70}$$

where ε and ϱ are in cgs. This reaction has been notoriously uncertain by factors of 2 and 3 at stellar temperatures. This has severe consequences for the production of carbon and even for the evolution of stars. The rate has been changed repeatedly within this uncertainty range as a result of new measurements. Kunz et al. (2002) provide the most recent analytical fit.

In each reaction $^{16}\mathrm{O}\ (\alpha,\gamma)\ ^{20}\mathrm{Ne}$, an energy of 4.73 MeV is released. The rate is according to Angulo et al. (1999):

$$\begin{aligned} \varepsilon_{16,\alpha} \approx \; & X_{16} X_4 \varrho f_{16,4} \cdot 1.91 \times 10^{27} T_9^{-2/3} \exp\left(-39.760 T_9^{-1/3} - (T_9/1.6)^2 \right) \\ & + 3.64 \times 10^{18} T_9^{-3/2} \exp(-10.32/T_9) \\ & + 4.39 \times 10^{19} T_9^{-3/2} \exp(-12.200/T_9) \\ & + 2.92 \times 10^{16} T_9^{2.966} \exp(-11.900/T_9) \; , \end{aligned} \tag{18.71}$$

where ε and ϱ are in cgs; this rate is also very uncertain.

Summarizing, we can say that during helium-burning reactions, (18.66) and (18.69) occur simultaneously, and the total energy generation rate is given by $\varepsilon_{\mathrm{He}} = \varepsilon_{3\alpha} + \varepsilon_{12,\alpha} + \varepsilon_{16,\alpha}$. If the initial ^{4}He is transformed into equal amounts of ^{12}C and ^{16}O, then the energy yield is $7.28 \times 10^{17}\,\mathrm{erg\,g^{-1}}$.

The general course of helium burning is always according to the following scheme: initially, when burning sets in at temperatures around 10^8 K, the triple-α reaction is dominating, both because of a larger cross section and of the carbon and oxygen abundances, which are low in comparison to that of helium. With progressing conversion of helium to carbon, the $^{12}C(\alpha,\gamma)^{16}O$ becomes more competitive. The increasing temperature is supporting this. When the helium content gets low, the fact that the triple-α reaction is proportional to the third power of the helium abundance disfavours it increasingly, such that the burning of carbon is larger than its creation by triple-α reactions, and its abundance decreases again, while simultaneously that of ^{16}O increases. The final abundances of ^{12}C and ^{16}O will thus depend on the competition between the reactions (18.69) and the exhaustion of ^{4}He particles. This depends mainly on the $^{12}C(\alpha,\gamma)^{16}O$ rate: if it is higher, the destruction of ^{12}C will set in earlier and a higher O:C ratio will result. Overall, the outcome of helium burning is O:C $\approx$ 1:1–2:1. Neon production is comparably unimportant.

18.5.3 Carbon Burning and Beyond

For a mixture consisting mainly of ^{12}C and ^{16}O (as would be found in the central part of a star after helium burning), *carbon burning* will set in if the temperature or the density rises sufficiently. The typical range of temperature for this burning is $T_8 \approx 5 \ldots 10$.

Here (and in the following types of burning) the situation is already so difficult that one often has to rely on rough approximations and guesses, or on complete nuclear networks. The first complication is that the original $^{12}C+^{12}C$ reaction produces an excited ^{24}Mg nucleus, which can decay via many different channels (the last column gives $Q/1$ MeV):

$$\begin{aligned} ^{12}C + {}^{12}C &\rightarrow {}^{24}Mg + \gamma \quad , \quad 13.931 \\ &\rightarrow {}^{23}Mg + n \quad , \quad -2.605 \\ &\rightarrow {}^{23}Na + p \quad , \quad 2.238 \\ &\rightarrow {}^{20}Ne + \alpha \quad , \quad 4.616 \\ &\rightarrow {}^{16}O + 2\alpha \, , \quad -0.114 \end{aligned} \tag{18.72}$$

The relative frequency of the channels is very different, and depends also on the temperature. The γ decay (leaving ^{24}Mg) is rather improbable, and the same is true for the two endothermic decays ($^{23}Mg + n$ and $^{16}O + 2\alpha$). The most probable reactions are those which yield $^{23}Na+p$ and $^{20}Ne+\alpha$. These are believed to occur at about equal rates for temperatures that are not too high (say $T_9 < 3$).

The next problem is that the produced p and α find themselves at temperatures extremely high for hydrogen and helium burning and will immediately react with some of the particles in the mixture (from ^{12}C up to ^{24}Mg). They may even start

whole reaction chains, such as $^{12}\mathrm{C}(p,\gamma)^{13}\mathrm{N}(e^+\nu)^{13}\mathrm{C}(\alpha,n)^{16}\mathrm{O}$, where the neutron could immediately react further. All these details would have to be evaluated quantitatively in order to find the average energy gain and the final products. For a rough guess one may assume that on average, $Q \approx 13\,\mathrm{MeV}$ are released per $^{12}\mathrm{C}$–$^{12}\mathrm{C}$ reaction (including all follow-up reactions). Then (Caughlan and Fowler 1988),

$$\begin{aligned}\varepsilon_{\mathrm{CC}} \approx\ & 1.86\times 10^{43} f_{\mathrm{CC}} \varrho X_{12}^2 T_9^{-3/2} T_{9a}^{5/6} \\ & \cdot \exp[-84.165/T_{9a}^{1/3} - 2.12\times 10^{-3} T_9^3] \end{aligned} \tag{18.73}$$

with ε and ϱ in cgs and with $T_{9a} = T_9/(1+0.0396T_9)$. The screening factor f_{CC} can become important (see Fig. 18.6), since this burning can start in very dense matter. The end products may be mainly $^{16}\mathrm{O}$, $^{20}\mathrm{Ne}$, $^{24}\mathrm{Mg}$, and $^{28}\mathrm{Si}$.

For *oxygen burning*, $^{16}\mathrm{O}+^{16}\mathrm{O}$, the Coulomb barrier is already so high that the necessary temperature is $T_9 \gtrsim 1$. As in the case of carbon burning, the reaction can proceed via several channels:

$$\begin{aligned} {}^{16}\mathrm{O} + {}^{16}\mathrm{O} &\rightarrow {}^{32}\mathrm{S} + \gamma\ , & 16.541 \\ &\rightarrow {}^{31}\mathrm{P} + p\ , & 7.677 \\ &\rightarrow {}^{31}\mathrm{S} + n\ , & 1.453 \\ &\rightarrow {}^{28}\mathrm{Si} + \alpha\ , & 9.593 \\ &\rightarrow {}^{24}\mathrm{Mg} + 2\alpha\ , & -0.393 \end{aligned} \tag{18.74}$$

Most frequent is the p decay, followed by the α decays. Again, all released p, n, and α are captured immediately, giving rise to a multitude of secondary reactions. Among the end products, one will find a large amount of $^{28}\mathrm{Si}$. For an average energy $Q \approx 16\,\mathrm{MeV}$ released per $^{16}\mathrm{O}+^{16}\mathrm{O}$ reaction, the energy generation rate is roughly

$$\begin{aligned}\varepsilon_{\mathrm{OO}} \approx\ & 2.14\times 10^{53} f_{\mathrm{OO}} \varrho X_{16}^2 T_9^{-2/3} \\ & \cdot \exp(-135.93/T_9^{1/3} - 0.629 T_9^{2/3} - 0.445 T_9^{4/3} + 0.0103 T_9^2) \end{aligned} \tag{18.75}$$

with ε and ϱ in cgs, and the screening factor f_{OO}.

For $T_9 > 1$, one also has to consider the possibility of *photodisintegration* of nuclei that are not too strongly bound. Here the radiation field contains a significant number of photons with energies in the MeV range, which can be absorbed by a nucleus, breaking it up, for example, by α decay. This is a complete analogue of photoionization of atoms, and, in equilibrium, a formula equivalent to the Saha formula [see (14.11)] holds for the number densities n_i and n_j of the final particles (after disintegration), relative to the number n_{ij} of the original (compound) particles:

$$\frac{n_i n_j}{n_{ij}} \sim T^{3/2} \mathrm{e}^{-Q/kT}\ , \tag{18.76}$$

where Q is the difference in binding energies between the original nucleus and its fragments. (Q corresponds to the ionization energy χ; however, it is about $10^2 \ldots 10^3$ times larger because of the much stronger nuclear forces.) The proportionality factor contains essentially the partition functions of the three types of particles. Equilibrium is usually not reached, and the details are very complicated and may differ from case to case, which is also true for the amount of energy released or lost.

The photodisintegration itself is, of course, endothermic. But the ejected particles (X_j) will be immediately recaptured. The capture can lead back to the original nucleus X_{ij}, i.e. the reaction would be $X_{ij} \rightleftarrows X_i + X_j$, or it can lead to quite different, even heavier, nuclei X_{jk} that are more strongly bound than the original one $X_j + X_k \rightarrow X_{jk}$. The latter case would be exothermic and can outweigh the endothermic photodisintegration in the total energy balance.

An example is *neon disintegration*, which in stellar evolution occurs even before oxygen burning:

$$^{20}\mathrm{Ne} + \gamma \rightarrow ^{16}\mathrm{O} + \alpha \,, \quad Q = -4.73\,\mathrm{MeV} \,. \tag{18.77}$$

It dominates over the inverse reaction (known from helium burning) at $T_9 > 1.5$. The ejected α particle reacts mainly with other ^{20}Ne nuclei, yielding $^{24}\mathrm{Mg}+\gamma$. The net result will then be the conversion of Ne into O and Mg:

$$2\,^{20}\mathrm{Ne} + \gamma \rightarrow \; ^{16}\mathrm{O} + ^{24}\mathrm{Mg} + \gamma \,, \quad Q = +4.583\,\mathrm{MeV} \,. \tag{18.78}$$

Another example is the photodisintegration of ^{28}Si, which may be the dominant reaction at the end of oxygen burning. Near $T_9 \approx 3$, ^{28}Si can be decomposed by the photons and eject n, p, or α. There follows a large number of reactions in which the thereby created nuclei (e.g. Al, Mg, Ne) will also be subject to photodisintegration, leading to the existence of an appreciable amount of free n, p, and α particles. These react with the remaining ^{28}Si, thus building up gradually heavier nuclei, until ^{56}Fe is reached. Since ^{56}Fe is so strongly bound, it may survive this melting pot as the only (or dominant) species. So, forgetting all intermediate stages, we would ultimately have the conversion of two ^{28}Si into ^{56}Fe, which can be called *silicon burning*.

For $T_9 \gtrsim 5$, photodisintegration breaks up even the ^{56}Fe nuclei into α particles and thus reverses the effect of all prior burnings. Such processes can occur during supernova explosions (see Chap. 36).

18.6 Neutron-Capture Nucleosynthesis

In Fig. 18.9 we show the solar abundances of elements. As on earth, we find all elements from hydrogen to lead and uranium in the Sun. The nuclear burning we discussed so far is able to produce only elements up to iron, since the creation of elements heavier than the "iron peak" is endothermic, and the electrostatic repulsion

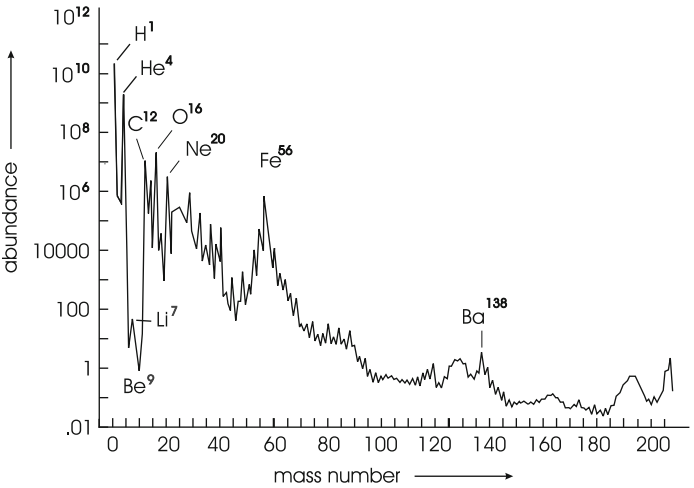

Fig. 18.9 The abundances (particle number fractions) of elements in the Sun, normalized to a value of 10^6 for ^{28}Si

for charged particle reactions is increasing with nuclear charge. The various peaks in this figure reflect the stability of isotopes against further addition of neutrons and protons and are due to the structure of the nuclei, easily explained in the shell model of nuclear physics. In particular isotopes with even and equal numbers of neutrons and protons, such as ^{12}C or ^{40}Ca, are very stable and therefore more abundant than neighbouring ones. If nuclear shells are closed, the stability is even higher, similar to the noble gases in atomic physics. Such isotopes are called "magic nuclei" with "magic" numbers of protons or neutrons. ^{16}O is a "double-magic" nucleus.

During hydrostatic burning phases, the elements beyond the iron peak can be produced only if other reactions with lighter nuclei provide enough energy and, most easily, if the reactions are processing by the capture of neutrons, since they are electrically neutral. Adding neutrons leads initially to heavier isotopes of the same element, which become the more unstable the more neutrons they have. The decay proceeds by emission of an electron, which is temperature-insensitive and therefore is acting as a kind of nuclear clock. β-decay times can reach from minutes to millions of years, and are getting shorter with increasing neutron excess. The decay leads to the creation of a new element of the same mass but with the charge being increased by one.

The general sequence of reactions is therefore

$$\begin{aligned}(Z, A) + n &\rightarrow (Z, A+1) + \gamma \\ (Z, A+1) &\rightarrow (Z+1, A+1) + e^- ,\end{aligned} \tag{18.79}$$

where the first reaction can be repeated several times, depending on the number density of available neutrons n and the neutron-capture cross section. If the

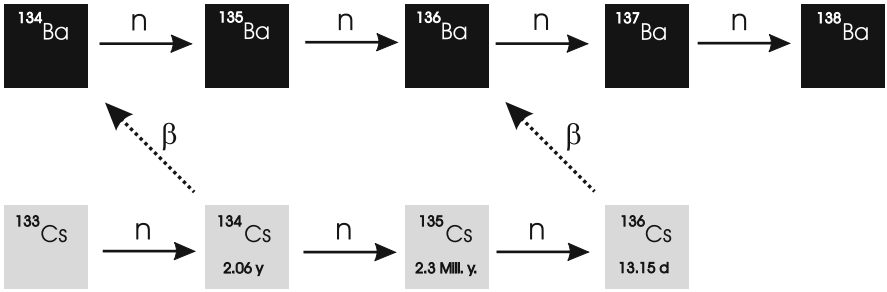

Fig. 18.10 Typical s-process reaction path in the nuclear chart, in the region of Cs and Ba. The laboratory half-life time of the Cs isotopes is given. It can be appreciable shorter at stellar temperatures. ^{134}Cs and ^{136}Cs are so-called branching points, and the relative abundances of isotopes in the various branches allow conclusions about the temperature at the s-process site (after Busso et al. 1999)

neutron-capture time is long compared to the β-decay time, the process is called the *slow neutron-capture process* or simply the *s-process*, and the reaction path remains close to the line of β-stability in the nuclear chart; if it is rapid, such that the first reaction in (18.79) is repeated several times, it is called the *r-process*. Subsequent neutron captures and β-decays will lead to the creation of the heavy elements. The astrophysical site for the r-process is not clearly identified, but is probably to be found in supernova explosions or similar energetic events. The s-process is certainly taking place in stars of intermediate mass ($M \approx 2 \cdots 5 M_\odot$) in an advanced phase of evolution (Sect. 34.3). In the atmospheres of such stars, short-lived isotopes of heavy elements (most importantly ^{99}Tc with a half-life time of only 211,000 years) have been found, which could only have been created in the stars themselves. Although the s-process may drain energy from the star, it is in fact unimportant for the energy budget and the structure of stars, mainly due to the extremely low abundances (see Fig. 18.9) with respect to the elements participating in the burning stages discussed earlier in this chapter. Figure 18.10 shows part of the s-process path in the Cs-Ba region of the nuclear chart. ^{138}Ba has a magic neutron number (82) and therefore is very stable and abundant (Fig. 18.9).

The necessary condition for the s- and r-process is the presence of neutrons. Since free neutrons are both unstable and are easily captured by other nuclei, a constant source of neutron production is needed. Considering the burning phases of Sect. 18.5, we realize that only protons and α-particles were involved. The generation of neutrons is indeed a very rare event in a star's life. However, in Sect. 18.5.3, we already mentioned that during carbon burning, the various reaction channels may lead to whole chains of subsequent reactions, one of them resulted in $^{13}\mathrm{C}(\alpha, n)^{16}\mathrm{O}$. Indeed, this is one of the two neutron sources identified, the other being $^{22}\mathrm{Ne}(\alpha, n)^{25}\mathrm{Mg}$, the end reaction of the sequence $^{14}\mathrm{N}(\alpha, \gamma)^{18}\mathrm{O}(\alpha, \gamma)^{22}\mathrm{Ne}$, which is operating at temperatures of about 4×10^8 K. Such temperatures are encountered during helium burning in massive stars, where the *neon source* may produce s-process elements.

The alternative *carbon source* for neutrons apparently requires the simultaneous presence of protons and α-particles as well as temperatures above 2×10^8 K for the α-capture. However, at these temperatures, usually all protons are already burnt to helium, and the amount of ^{13}C is very low, since the overwhelming carbon isotope is ^{12}C from helium burning. The solution is to bring fresh hydrogen into hot layers of freshly produced ^{12}C but to keep the abundance of protons so low that no further CNO processing to ^{14}N is happening. Such a situation can be achieved by complicated sequences of mixing processes between the helium-burning regions of a star of intermediate mass and its hydrogen-rich envelope. We will discuss this in Sect. 34.3. In full stellar models, the neutron densities achieved range from 10^6 to $10^{10}\,\mathrm{cm}^{-3}$.

The neutron-capture cross section is inversely dependent on velocity (or temperature):

$$\sigma \sim \frac{1}{v} , \tag{18.80}$$

therefore $\langle \sigma v \rangle$ in (18.21) is actually close to a constant (σv) times the integral over $f(E)$ and only slightly dependent on the stellar plasma temperature, except for nuclei close to magic neutron numbers, where σ may be lower by an order of magnitude or more. It generally lies in the range of 100 to 1000 mb (1 b = $10^{-24}\,\mathrm{cm}^2$).

We define

$$\langle \sigma \rangle := \langle \sigma(v) v \rangle / v_T , \tag{18.81}$$

where $v_T = (2kT/\mu_n)^{1/2}$ is the thermal velocity in the system of a nucleus A and a neutron n, μ_n being the reduced mass of it. $\langle \sigma \rangle$ corresponds approximately to the cross section measured at that relative velocity. The rate equation for a nucleus with mass A and density n_A is then

$$\frac{\mathrm{d}n_A}{\mathrm{d}t} = -\langle \sigma(v) v \rangle_A n_n n_A + \langle \sigma(v) v \rangle_{A-1} n_n n_{A-1} . \tag{18.82}$$

With (18.81) this becomes

$$\frac{\mathrm{d}n_A}{\mathrm{d}t} = v_T n_n (-\sigma_A n_A + \sigma_{A-1} n_{A-1}) . \tag{18.83}$$

Since the neutron density n_n may vary with time, we define

$$\mathrm{d}\tau = v_T n_n(t) \mathrm{d}t, \tag{18.84}$$

so we obtain

$$\frac{\mathrm{d}n_A}{\mathrm{d}\tau} = -\sigma_A n_A + \sigma_{A-1} n_{A-1} . \tag{18.85}$$

This equation is self-regulating: assume that initially n_A is very small. Then n_A will grow due to the positive second term in (18.85). This will also increase the first

term until the right-hand side vanishes and n_A has reached a stationary value. The abundances of A and $A-1$ will therefore reflect the ratio of cross sections σ_A and σ_{A-1}. The integral over $\mathrm{d}\tau$,

$$\tau = v_T \int n_n(t)\mathrm{d}t, \tag{18.86}$$

is called the *neutron exposure* and reflects the integrated flux of neutrons with thermal velocities. Its dimension is that of an inverse area and typically of order mb^{-1}. It is the decisive quantity determining the overall abundances of elements produced by neutron captures, and how far the s- or r-process can proceed. The relative abundances of isotopes produced then reflect the cross section σ.

The synthesis of neutron-capture elements has to be computed with huge nuclear networks consisting of hundreds of isotopes and even more reactions. Simplified models assuming a distribution of neutron exposures on a single initial *seed nucleus*, usually ^{56}Fe, can quite successfully reproduce the solar abundance patterns. This distribution $\rho(\tau)$ is

$$\rho(\tau) = \frac{f n_{56}}{\tau_0} \exp(-\tau/\tau_0)\ , \tag{18.87}$$

with f and τ_0 being two free parameters. With (18.87) the rate equation (18.85) can be solved analytically for nucleus A:

$$\sigma_A n_A = \frac{f n_{56}}{\tau_0} \prod_{i=56}^{A} \left[1 + (\sigma_i \tau_0)^{-1}\right]^{-1} \tag{18.88}$$

More details about neutron-capture nucleosynthesis for the interested reader can be found in the reviews by Meyer (1994), Arnould and Takahashi (1999), and Busso et al. (1999).

18.7 Neutrinos

Neutrinos require special consideration because their cross section σ_ν for interaction with matter is so extremely small. For scattering of neutrinos with energy E_ν, one has roughly $\sigma_\nu \approx (E_\nu/m_\mathrm{e}c^2)^2 10^{-44}\,\mathrm{cm}^2$. Neutrinos in the MeV range then have $\sigma_\nu \approx 10^{-44}\,\mathrm{cm}^2$, which is a factor 10^{-18} smaller than the cross section for typical photon–matter interactions. The corresponding mean free path in matter of density $\varrho = n\mu m_\mathrm{u}$ and molecular weight $\mu(\approx 1)$ is about

$$\ell_\nu = \frac{1}{n\sigma_\nu} = \frac{\mu m_\mathrm{u}}{\varrho\sigma_\nu} \approx \frac{2\times 10^{20}\mathrm{cm}}{\varrho}\ , \tag{18.89}$$

with ϱ in cgs. For "normal" stellar matter with $\varrho \approx 1\,\mathrm{g\,cm^{-3}}$, (18.89) would give a mean free path of the neutrinos of $\ell_\nu \approx 100\,\mathrm{parsec}$, and even for $\varrho = 10^6\,\mathrm{g\,cm^{-3}}$, one has $\ell_\nu \approx 3000\,R_\odot$.

Therefore it is safe to say that neutrinos, once created somewhere in the central region, leave a normal star without interactions carrying away their energy. This neutrino energy has then to be excluded from all other forms of energies (e.g. that released by nuclear reactions), which are subject to some diffusive transport of energy according to the temperature gradient.

The situation can be completely different, however, during a collapse in the final evolutionary stage. The density can reach nuclear values, and for $\varrho = 10^{14}\,\mathrm{g\,cm^{-3}}$, (18.89) gives only $\ell_\nu \approx 20\,\mathrm{km}$. Considering the fact that neutrinos can then be rather energetic (which increases σ_ν appreciably) one sees that many of them will be reabsorbed within the star. Then it is necessary to consider a transport equation for neutrino energy and to evaluate the amount of momentum the interacting neutrinos deliver to the overlying layers (see Sect. 36.3.3).

Only electron neutrinos play a role in stellar interiors, and these can be created in quite different processes inside a star. We first recall those processes involving nuclear reactions, which have already been mentioned (Sect. 18.5) in connection with certain nuclear burnings. In this special case one usually allows for the neutrino energy loss by a corresponding reduction of the released energy [This means that in (10.3) ε_n is reduced and no separate ε_ν term is needed.].

We already encountered this situation in the case of hydrogen burning (Sect. 18.5.1), where two neutrinos per fresh helium nucleus are created. The energy loss due to the escaping neutrinos depends on the particular chain or cycle by which the burning proceeds, but on average the energy yield per cycle is 25 MeV or $\approx 4 \times 10^{-5}$ erg. The generation of one solar luminosity ($L_\odot \approx 4 \times 10^{33}\,\mathrm{erg\,s^{-1}}$) by hydrogen burning implies thus a production of about 2×10^{38} neutrinos per second. Those neutrinos coming directly from the central region of the Sun yield a flux of roughly 10^{11} neutrinos per $\mathrm{cm^2}$ each second at the distance of earth. For experiments measuring the *solar neutrinos* see Sect. 29.5.

There are also neutrino-producing nuclear reactions that are not connected with nuclear burnings. For example, at extreme densities, degenerate electrons can be pushed up to energies large enough for *electron capture* by protons in nuclei of charge Z and atomic weight A : $e^- + (Z, A) \rightarrow (Z-1, A) + \nu$.

Another interesting example is the so-called *Urca process*. For a suitable nucleus (Z, A), an electron capture occurs which is followed by β decay:

$$\begin{aligned} (Z, A) + e^- &\rightarrow (Z-1, A) + \nu\ , \\ (Z-1, A) &\rightarrow (Z, A) + e^- + \bar{\nu}\ . \end{aligned} \tag{18.90}$$

The original particles are restored, and two neutrinos are emitted. There are obvious restrictions on the nuclei (Z, A) suitable for this process: they must have an isobaric nucleus $(Z-1,\ A)$ of slightly higher energy that is unstable to β decay. A possible example would be ^{35}Cl $(e^-, \nu)^{35}$S (endothermic with $Q = -0.17\,\mathrm{MeV}$), followed

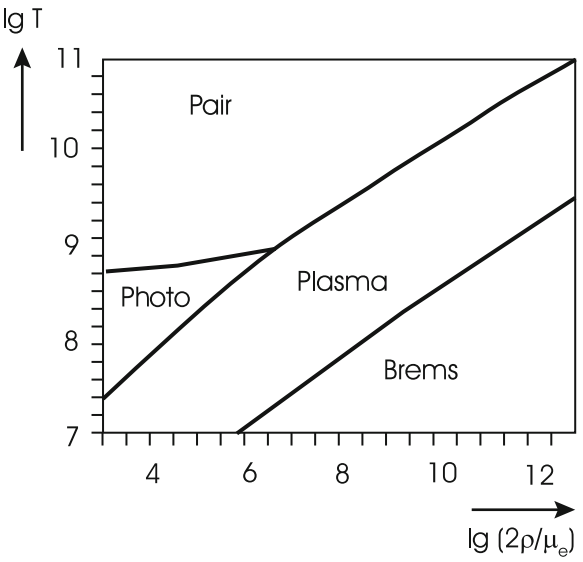

Fig. 18.11 Regions in which different types of neutrino less dominate. The lines indicate where neighbouring processes contribute approximately in equal shares. $2\varrho/\mu_e$ is a suitable quantity proportional to the electron density. It is identical to the mass density if $\mu_e = 2$, for example, in helium cores (After Haft et al. 1994)

by the decay $^{35}\mathrm{S}\ (e^-\bar{\nu})^{35}\,\mathrm{Cl}$, the energy for the first reaction being supplied by the captured electron. In this way, thermal energy of the stellar matter is converted into neutrino energy and lost from the star, while the composition remains unchanged (*Urca* is the name of a Rio de Janeiro casino, where Gamow and Schönberg found that, as the only recognizable net effect, similar losses, little by little, occur with visitors' money.). Details depend very much on the stellar material. If appropriate nuclei for this are present, the energy loss will increase with ϱ and T.

The following processes occur *without a nuclear reaction*. These purely leptonic processes were predicted as a consequence of the generalized Fermi theory of weak interaction, which allows a direct electron–neutrino coupling, such that a neutrino pair can be emitted if an electron changes its momentum. It is clear that such processes may be reduced by degeneracy if the electrons do not find enough free cells in phase space.

Several processes of this type can be important for stellar interiors. Figure 18.11 shows the approximate regions of the $\varrho - T$ plane where this is the case. Generally, the energy loss rates are complicated functions of density and temperature. They are calculated from theories of weak interaction and the results obtained as tables, for which approximative analytical fitting formulae are derived, which themselves are too complicated to be reproduced here. A compilation of results is given by Itoh et al. (1996); a somewhat simpler fitting formula for plasma neutrinos was derived by Haft et al. (1994).

Pair Annihilation Neutrinos: $e^- + e^+ \rightarrow \nu + \bar{\nu}$ In very hot environments ($T_9 > 1$), there are enough energetic photons to create large numbers of (e^-e^+) pairs. These will soon be annihilated, usually giving two photons, and a certain equilibrium abundance of e^+ will be reached. In this continuous back and forth

exchange, however, there is a small one-way leakage, since roughly once in 10^{19} times, the annihilation results in a pair $(\nu\bar{\nu})$ instead of the usual photons. This can lead to appreciable energy loss only in a very hot, not too dense plasma. ε_ν is a complicated function, but is always proportional to ϱ^{-1}.

Photoneutrinos: $\gamma + e^- \to e^- + \nu + \bar{\nu}$ This is the analogue of normal Compton scattering, in which a photon is scattered by an electron. In very few cases it may happen that, after scattering, the photon is replaced by a neutrino–antineutrino pair. The rates of energy loss for this process are rather different for different limiting cases (depending on the degrees of degeneracy and the importance of relativistic effects).

Plasmaneutrinos: $\gamma_{\rm plasm} \to \nu + \bar{\nu}$ A so-called plasmon decays here to a neutrino–antineutrino pair. The plasma frequency ω_0 is given by

$$\omega_0^2 \frac{m_{\rm e}}{4\pi e^2 n_{\rm e}} = \begin{cases} 1 & \text{, non-degenerate} \\ \left[1 + \left(\frac{\hbar}{m_{\rm e}c}\right)^2 (3\pi^2 n_{\rm e})^{2/3}\right]^{-1/2} & \text{, degenerate .} \end{cases} \tag{18.91}$$

This is important for an electromagnetic wave of frequency ω moving through the plasma, since its dispersion relation is

$$\omega^2 = K^2 c^2 + \omega_0^2 \,, \tag{18.92}$$

where K is the wave number. Here the wave is coupled to the collective motions of the electrons, and a propagating wave can occur only for $\omega > \omega_0$. Multiplication of (18.92) by $\hbar^2$ gives the square of the energy E of a quantum, which therefore behaves as if it were a relativistic particle with a rest mass corresponding to the energy $\hbar\omega_0$. Such a quantum is called a *plasmon.* For the energy rate, one has to add the rates of transversal and longitudinal plasmons: $\varepsilon_\nu^{(\rm plasm)} = \varepsilon_\nu^t + \varepsilon_\nu^l$. The emission rate has an exponential decrease for large ω_0, which is proportional to $\varrho^{1/2}$ at constant T. This comes from the fact that very few plasmons can be excited if kT drops below $\hbar\omega_0$.

Bremsstrahlung Neutrinos Inelastic scattering (deceleration) of an electron in the Coulomb field of a nucleus will usually lead to emission of a "Bremsstrahlung" photon (free–free emission). This photon can be replaced by a neutrino–antineutrino pair. The rate of energy loss for very large ϱ is

$$\varepsilon_\nu^{(\rm brems)} \approx 0.76 \frac{Z^2}{A} T_8^6 \,, \tag{18.93}$$

(in cgs) where Z and A are the charge and mass number of the nuclei. For smaller densities ε_ν is smaller than this expression, the correction being roughly a factor 10 at $\varrho \approx 10^4\,{\rm g\,cm^{-3}}$. This process can dominate, in particular, at low temperature and

very high density. The rate $\varepsilon_\nu^{(\mathrm{brems})}$ does not decrease with increasing degeneracy (as other processes do), since the lack of free cells in phase space is compensated by an increasing cross section for neutrino emission.

Synchrotron Neutrinos These can only occur in the presence of strong magnetic fields. The normal synchrotron photon emitted by an electron moving in this field is again replaced by a neutrino–antineutrino pair.